Carbohydrate Research, 230 (1992) 299–318
Elsevier Science Publishers B.V., Amsterdam

Synthesis and conformational and NMR studies of α-D-mannopyranosyl and α-D-mannopyranosyl-(1 → 2)-α-D-mannopyranosyl linked to L-serine and L-threonine

Anne Helander [a], Lennart Kenne [b], Stefan Oscarson [c], Thomas Peters [d] and Jean-Robert Brisson [e]

[a] *Kabi Pharmacia Therapeutics, Urology / Gynaecology, S-112 87 Stockholm (Sweden)*
[b] *Department of Chemistry, Swedish University of Agricultural Sciences, Box 7015, S-750 07 Uppsala (Sweden)*
[c] *Department of Organic Chemistry, Arrhenius Laboratory, Stockholm University, S-106 91 Stockholm (Sweden)*
[d] *University of Frankfurt, Institute of Biophysical Chemistry, Theodor-Stern-Kai 7-15, D-6000 Frankfurt / M.70 (Germany)*
[e] *National Research Council, Institute for Biological Sciences, 100 Sussex Drive, Ottawa, Ontario, K1A 0R6 (Canada)*

(Received September 18th, 1991; accepted December 3rd, 1991)

ABSTRACT

α-D-Mannopyranosyl and α-D-mannopyranosyl-(1 → 2)-α-D-mannopyranosyl linked to L-serine and L-threonine have been synthesised as model substances for the linkage region in certain O-linked glycoproteins. Metropolis Monte Carlo simulations were performed with a modified version of the GESA program, to yield theoretical NOEs and interatomic distances as ensemble-average values, and these were compared with results from steady-state NOE experiments. The NOEs were determined as ensemble-average and as global minimum values. NMR chemical shift differences, obtained for signals of the glycopeptides relative to those of the respective monomers, were interpreted in terms of short inter-residue atomic distances as found within the global minima, and on the basis of averaged distances derived from Monte Carlo simulations.

INTRODUCTION

The most widespread species of O-linked glycoproteins carry 2-acetamido-2-deoxy-D-galactopyranosyl residues linked to L-serine or L-threonine residues[1]. Another type of O-linkage consists of α-D-mannopyranosyl residues bound to the same amino acids and is found mainly in glycoproteins from yeasts and molds[1]. This class of compounds has also been found in glucoamylase G1 from *Aspergillus niger*[2] and in the glycosylated variant of human insulin-like growth factor I (IGF-I)

Correspondence to: Professor L. Kenne, Department of Chemistry, Swedish University of Agricultural Sciences, Box 7015, S-750 07 Uppsala, Sweden.

expressed in *Saccharomyces cerevisiae*[3]. The glycosylated variant of IGF-I was found to have mainly the disaccharide α-D-Man*p*-(1 → 2)-α-D-Man*p*-(1 → linked to an L-threonine residue.

There is an interest in using yeasts in the production of recombinant proteins for pharmacological applications. Thus, knowledge about possible glycosylations and their consequences for the biological activity is needed. NMR spectroscopy is one of the main tools in structural studies of glycopeptides and it has been demonstrated that chemical shift data can be used to reveal certain structural properties[4]. Knowledge about inter-residue ^1H–^1H-interactions, observed as NOEs, aids sequence analysis and gives important information on the conformational properties of saccharides[5].

We now report on the synthesis of α-D-mannopyranosyl and α-D-mannopyranosyl-(1 → 2)-α-D-mannopyranosyl linked to L-serine (**1** and **3**) and L-threonine (**2** and **4**), and on conformational and NMR studies of these compounds. Recently, a similar synthesis of the same disaccharide linked to L-threonine was published[6] and this element was then used in the synthesis of a pentadecapeptide.

EXPERIMENTAL

General methods.—These were as described earlier[7].

Fmoc-O-(2,3,4,6-tetra-O-acetyl-α-D-mannopyranosyl)-L-serine benzyl ester * (**5**). —A solution of silver triflate (0.30 g) in toluene (2 mL) was added at 0° to a mixture of Fmoc-L-serine benzyl ester[8] (0.30 g) and 2,3,4,6-tetra-*O*-acetyl-D-mannopyranosyl chloride[9] (0.33 g) in CH_2Cl_2 (5 mL) containing molecular sieves (4A). The mixture was allowed to attain room temperature and left for an additional hour before subjecting it to silica gel chromatography. Elution with 4:1 toluene–EtOAc gave **5** (0.47 g, 89%), $[\alpha]_D$ + 29° (*c* 0.6, $CHCl_3$). ^{13}C-NMR data ($CDCl_3$): δ 170.5, 169.8, 169.7, 169.4, 155.8, 143.7, 141.3, 135.0, 129.0–127.1, 125.1, 120.0, 98.6, 69.7, 69.3, 69.2, 68.8, 67.7, 67.3, 65.9, 62.3, 54.5, 47.1, 20.8, and 20.6.

Anal. Calcd for $C_{39}H_{42}NO_{14}$: C, 62.6; H, 5.6; N, 1.9. Found: C, 62.8; H, 5.3; N, 1.7.

O-α-D-*Mannopyranosyl*-L-*serine* (**1**).—A solution of **5** (0.33 g) in morpholine (3 mL) was stirred at room temperature for 30 min. Dichloromethane (30 mL) was added, and the mixture was washed with H_2SO_4 (0.05 M) and water, dried, and concentrated. The residue was purified on a column of silica gel ($CHCl_3$–acetone, 4:1) to give 2,3,4,6-tetra-*O*-acetyl-α-D-mannopyranosyl-L-serine benzyl ester (0.14 g, 60%). This derivative was dissolved in MeOH (10 mL) containing Pd–C (10%) and hydrogenolysed at 400 kPa for 5 h. The catalyst was filtered off and hydrazine hydrate (2 mL) was added at room temperature to the stirred filtrate. After 2 h, the solution was cooled to 0°, acetone (15 mL) was added, and stirring was

* Fmoc = *N*-9-fluorenylmethyl chloroformate derivative.

continued for 30 min. The solvents were evaporated and the residue was dissolved in MeOH. Acetone was added, and the precipitate was filtered off and purified on a column of Bio-Gel P-2, to give **1** (60 mg, 51% from **5**, 84% from the deFmoc derivative), $[\alpha]_D$ +58° (*c* 0.9, H_2O); lit.[10] $[\alpha]_D$ +20° (*c* 1.0, H_2O).

Fmoc-O-(2,3,4,6-tetra-O-acetyl-α-D-mannopyranosyl)-L-threonine benzyl ester (**6**).—Compound **6** was prepared as described above for **5**, except that Fmoc-L-threonine benzyl ester[11] (0.30 g) was used instead. Compound **6** (0.48 g, 90%) had $[\alpha]_D$ +34° (*c* 1.1, $CHCl_3$). ^{13}C-NMR data ($CDCl_3$): δ 169.8, 156.7, 143.9, 143.7, 141.3, 135.0, 129.0–127.1, 125.2, 120.0, 98.8, 69.9, 69.1, 68.7, 67.8, 67.5, 66.3, 62.5, 58.7, 47.1, 20.8, 20.6, and 17.9.

Anal. Calcd for $C_{40}H_{44}NO_{14}$: C, 63.0; H, 5.8; N, 1.8. Found: C, 62.9; H, 5.8; N, 1.7.

O-*α*-D-*Mannopyranosyl*-L-*threonine* (**2**).—Compound **6** (0.35 g) was deprotected, as described above for derivative **5**, to give **2** (90 mg, 70%), $[\alpha]_D$ +41° (*c* 1.0, H_2O); lit.[10] $[\alpha]_D$ +16° (*c* 0.7, H_2O).

Ethyl 2,3,4,6-tetra-O-benzyl-1-thio-α-D-mannopyranoside (**7**).—Benzyl bromide (3 g) was added to a mixture of ethyl 1-thio-α-D-mannopyranoside[12] (0.48 g) and NaH (0.43 g) in *N*,*N*-dimethylformamide (10 mL). After 4 h, the mixture was cooled to 0°, MeOH (10 mL) was added, and the mixture was concentrated. The residue was purified on a column of silica gel (toluene–EtOAc, 20:1) to give **7** (1.18 g, 94%), $[\alpha]_D$ + 64° (*c* 0.9, $CHCl_3$). ^{13}C-NMR data ($CDCl_3$): δ 138.5, 138.3, 138.2, 138.1, 128.3–127.4, 81.8, 80.3, 76.4, 75.0, 73.3, 72.0, 71.9, 69.1, 25.2, and 14.9.

Anal. Calcd for $C_{36}H_{40}O_5S$: C, 73.9; H, 6.9; S, 5.5. Found: C, 73.7; H, 6.9; S, 5.3.

Ethyl 3,4,6-tri-O-benzyl-1-thio-α-D-mannopyranoside (**8**).—Zinc chloride (1 g) was added to a solution of 1,2-di-*O*-acetyl-3,4,6-tri-*O*-benzyl-D-mannopyranose[13] (1.5 g) and ethanethiol (0.3 mL) in CH_2Cl_2. After 15 min, the mixture was diluted with CH_2Cl_2 (40 mL), washed with aq $NaHCO_3$ and water, dried (Na_2SO_4), and concentrated. The residue was separated on a column of silica gel (toluene–EtOAc, 14:1) to give ethyl 2-*O*-acetyl-3,4,6-tri-*O*-benzyl-1-thio-α-D-mannopyranoside (1.1 g, 67%) slightly contaminated with the β anomer and starting material (0.3 g, 19%). Sodium methoxide in MeOH (1 M, 1 mL) was added to a solution of the thiosaccharide (1.0 g) in MeOH (10 mL), and the mixture was stirred at room temperature overnight. Acetic acid (100 μL) was added, the mixture was concentrated, and the residue was fractionated on a column of silica gel (toluene–EtOAc, 9:1) to give **8** (0.85 g, 92%), $[\alpha]_D$ + 126° (*c* 0.9, $CHCl_3$). ^{13}C-NMR data ($CDCl_3$): δ 138.3, 138.2, 137.7, 128.5–127.5, 83.4, 80.4, 75.0, 74.5, 73.3, 72.9, 71.4, 69.8, 68.9, 24.8, and 14.8.

Anal. Calcd for $C_{29}H_{34}O_5S$: C, 70.4; H, 6.9; S, 6.5. Found: C, 70.4; H, 6.8; S, 6.5.

Ethyl 3,4,6-tri-O-benzyl-2-O-(2,3,4,6-tetra-O-benzyl-α-D-mannopyranosyl)-1-thio-α-D-mannopyranoside (**9**).—Bromine (100 μL) was added to a solution of **7** (1.25 g) in CH_2Cl_2 (10 mL) at 0°. After 15 min, cyclohexene (75 μL) was added and, after an additional 5 min, the mixture was concentrated to give crude 2,3,4,6-tetra-*O*-

benzyl-D-mannopyranosyl bromide, which was used in the following coupling reaction without further purification.

A solution of silver triflate (0.63 g) in toluene (4 mL) was added dropwise at −30° to a solution of the above bromide, the thioglycoside derivative **8** (0.69 g), and collidine (200 μL) in CH_2Cl_2 (10 mL) containing molecular sieves (4A). After 30 min, when the mixture had reached −10°, aq sodium thiosulfate (10%, 5 mL) was added, and the mixture was allowed to attain room temperature. Dichloromethane (40 mL) and water (20 mL) were added and the two phases separated. The organic phase was dried (Na_2SO_4) and concentrated, and the residue was purified on a column of silica gel (toluene–EtOAc, 25:1) to yield **9** (1.1 g, 80%), $[\alpha]_D$ +49° (*c* 0.4, $CHCl_3$). ^{13}C-NMR data ($CDCl_3$): δ 138.5, 138.4, 138.3, 138.0, 128.5–127.4, 99.7, 83.8, 80.3, 79.7, 76.4, 75.1, 75.0, 74.9, 73.2, 72.4, 72.3, 72.2, 69.5, 69.2, 25.5, and 15.0.

Anal. Calcd for $C_{63}H_{68}O_{10}S$: C, 74.4; H, 6.7; S, 3.1. Found: C, 73.9; H, 6.4; S, 3.0.

Fmoc-O-[3,4,6-tri-O-benzyl-2-O-(2,3,4,6-tetra-O-benzyl-α-D-mannopyranosyl)-α-D-mannopyranosyl]-L-serine benzyl ester (**10**).—Methyl triflate (75 μL) was added at room temperature to a solution of **9** (0.21 g) and Fmoc-L-serine benzyl ester (0.10 g) in CH_2Cl_2 (5 mL) containing molecular sieves (4A), and the mixture was stirred overnight. Pyridine (100 μL) was added, whereafter the mixture was fractionated on a column of silica gel (toluene–EtOAc, 19:1), to give **10** (0.21 g, 75%), $[\alpha]_D$ +17° (*c* 0.6, $CHCl_3$), and the β anomer (0.04 g, 14%). ^{13}C-NMR data for **10** ($CDCl_3$): δ 169.8, 156.0, 143.8, 141.2, 138.6, 138.4, 138.3, 138.2, 135.4, 128.6–127.1, 125.2, 119.9, 100.0, 99.9, 79.7, 79.4, 75.1, 74.9, 74.8, 74.5, 73.3, 72.5, 72.3, 72.2, 69.7, 69.3, 69.1, 67.2, 54.6, and 47.1.

Anal. Calcd for $C_{86}H_{86}NO_{15}$: C, 75.2; H, 6.3; N, 1.0. Found: C, 75.0; H, 6.0; N, 0.8.

O-*(2-O-α-D-Mannopyranosyl-α-D-mannopyranosyl)-L-serine* (**3**).—Compound **10** (0.18 g) was deprotected as described below for **11**, except that no chromatographic purification was made after the Fmoc deprotection step, to give **3** (40 mg, 71%), $[\alpha]_D$ +66° (*c* 0.6, H_2O).

Anal. Calcd for $C_{15}H_{27}NO_{13} \cdot 1.5H_2O$: C, 39.5; H, 6.6; N, 3.1. Found: C, 39.5; H, 6.2; N, 3.0.

Fmoc-O-[3,4,6-tri-O-benzyl-2-O-(2,3,4,6-tetra-O-benzyl-α-D-mannopyranosyl)-α-D-mannopyranosyl]-L-threonine benzyl ester (**11**).—Compound **11** was prepared from Fmoc-L-threonine benzyl ester (0.15 g) and **9** (0.24 g), as described above for **10**. Compound **11** (0.26 g, 80%) had $[\alpha]_D$ +24° (*c* 1.3, $CHCl_3$). ^{13}C-NMR data ($CDCl_3$): δ 170.3, 156.5, 143.8, 143.7, 141.2, 138.6, 138.4, 138.2, 138.1, 135.2, 128.0–127.1, 125.1, 119.9, 100.2, 99.8, 79.8, 79.2, 75.3, 74.9, 74.7, 73.3, 72.3, 72.2, 69.5, 69.2, 67.2, 58.8, 47.2, and 18.1.

Anal. Calcd for $C_{87}H_{88}NO_{15}$: C, 75.3; H, 6.4; N, 1.0. Found: C, 74.2; H, 6.3; N, 1.0.

O-*(2-O-α-D-Mannopyranosyl-α-D-mannopyranosyl)-L-threonine* (**4**).—The Fmoc-

group was removed from **11** (0.22 g), as described above for **5**, to give an intermediate (0.17 g, 92%) which was dissolved in MeOH–acetic acid–water (4:1:1, 40 mL) and hydrogenolysed over Pd–C (10%) at 400 kPa overnight. The filtered solution was concentrated, diluted with water, washed with CH_2Cl_2 and EtOAc, and concentrated. The residue was purified on a column of Bio-Gel P-2, eluted with water, and lyophilised to give **4** (48 mg, 69% from **11**), $[\alpha]_D$ +52° (*c* 0.6, H_2O).

Anal. Calcd for $C_{16}H_{29}NO_{13} \cdot 2H_2O$: C, 40.1; H, 6.9; N, 3.3. Found: C, 39.8; H, 6.3; N, 2.9.

NMR spectroscopy.—The ^1H- and ^{13}C-NMR spectra were recorded for solutions at 30° with JEOL GSX-270 and GX-400 instruments. The substances were dissolved in D_2O, using acetone (δ_H 2.225) and 1,4-dioxane (δ_C 67.40) as internal references. The solutions had a pD of 4–6. In this region, only minor shifts (< 0.01 ppm) of signals from the amino acid residues occurred. The signals were assigned by a combination of 1D NMR spectra and different 2D H,H- and C,H-COSY experiments. NOE difference experiments were performed with pre-irradiation for 5 s at the frequency of the selected protons, using the NOEDIF pulse sequence available from the JEOL standard software. The absolute enhancements were calculated as % relative to the irradiated signal, and the relative NOEs as the ratio of two NOEs ×100, where the NOE value from the intramolecular H-1 and H-2 interaction was always used as the reference value.

Computational methods.—All calculations were performed on a CONVEX C120 computer. Potential energy calculations were performed on compounds **3** and **4**, using a modified version of the GESA program[14,15] that embodies the HSEA approach[16,17], assuming that the main forces determining the conformation of oligosaccharides are van der Waals interactions and the exo-anomeric effect[18,19]. The modifications of the GESA program include the implementation of a Metropolis Monte Carlo (MMC) simulation routine[20] that allows the prognosis of ensemble-average[21–24] NOE enhancements, ⟨NOE⟩s. Co-ordinates for L-serine and L-threonine were obtained via model building with INSIGHT (Biosym Technologies), based upon X-ray co-ordinates of α-D-Man*p*-(1 → O)-L-Thr[25]. Hydrogen atoms were deleted and replaced with standard geometry. Co-ordinates for the α-D-mannopyranosyl residues were taken from neutron diffraction data[26]. In the following text, atoms belonging to the amino acid residues are designated α, β, and γ, those of the mannopyranosyl residues linked to the amino acid are unprimed, and atoms of the second mannopyranosyl group are primed. Dihedral angles at the glycosidic linkages, the C-5–C-6 axes and the Cα–Cβ bonds are defined as follows: ϕ_1 H-1′–C-1′–O-1′–C-2; ψ_1 C-1′–O-1′–C-2–H-2; ϕ_2 H-1–C-1–O-1–Cβ; ψ_2 C-1–O-1–Cβ–Cα; ω_1 O-5′–C-5′–C-6′–O-6′; ω_2 O-5–C-5–C-6–O-6; and χ O-1–Cβ–Cα–Nα. MMC calculations followed the protocol published[20]. Two sets of MMC simulations were performed. In one treatment, all dihedral angles ϕ, ψ, ω, and χ were considered to be variable, resulting in a seven-dimensional energy hyperspace for each disaccharide peptide. The other treatment

utilised fixed χ angles for the side-chain orientations of L-serine and L-threonine, resulting in a six-dimensional energy hyperspace for each disaccharide peptide. In these simulations, the angle χ was set at 60°, resulting in an ideal staggered conformation of the Cα–Cβ bond. A similar value for χ was found in the crystal structure of α-D-Man*p*-(1 → O)-L-Thr[25]. Vicinal coupling constants $J_{H\alpha,H\beta(H\beta')}$ also indicated the preference of conformers with χ angles near 60° (see discussion below). The values for the coupling constants $J_{H\alpha,H\beta}$, $J_{H\alpha,H\beta'}$ were 3.0, 5.4 Hz and 3.0, 6.0 Hz for the L-serine compounds **1** and **3**, respectively. For the L-threonine compounds **2** and **4**, $^3J_{H\alpha,H\beta}$ values of 2.7 and 3.0 Hz, respectively, were found. Since variation of χ during the MMC simulations applied no extra torsional potential function taking into account the charged substituents at Cα, only $\langle NOE \rangle_{MMC}$ values derived from the simulations with χ fixed at 60° were compared to the experimental NOEs. All simulations were preceded by 2000 macromove equilibration periods. Starting with the global minimum conformations, MMC simulations were performed comprising 250000 macro steps with the temperature parameter set at 300 or 310 K. For the L-threonine-linked disaccharide **4**, one simulation was carried out with the temperature parameter set at 900 K. Step lengths of 10° for all angles were used for the first set of simulations with χ variable, resulting in overall acceptance ratios of 0.54 and 0.42 for **3** and **4**, respectively. The simulation of **4** at 900 K applied step lengths of 20°, giving rise to an overall acceptance ratio of 0.39. For the MMC simulations with χ fixed at 60°, step lengths were set at 15° for glycosidic linkages and 20° for C-5–C-6 bonds, yielding overall acceptance ratios of 0.38 for **3** and 0.30 for **4**. Local acceptance ratios were monitored for the whole course of the simulations, indicating a stable behaviour of the systems under investigation. Ensemble-average NOEs, denoted as $\langle NOE \rangle_{MMC}$ were then derived from the MMC calculations utilising either $\langle r^{-6} \rangle_{MMC}$ or $\langle r^{-3} \rangle^2_{MMC}$ values[21], with r being the distances between protons. Calculation of NOEs for the global minima was performed on the basis of r^{-6} values, with r being the inter-proton distances within the minimum energy conformation. Both NOE and $\langle NOE \rangle_{MMC}$ values were calculated employing the full relaxation matrix approach[27,28], as this has been discussed in detail in previous studies[20,21,24]. A spectrometer frequency of 400 MHz was used for the theoretical NOE calculations. Overall motional correlation times were fitted to the experimentally derived NOE values[29] and finally set at 2.4×10^{-10} s. Internal rotations of the L-threonine methyl group were taken into account by the three-state jump model employing internal correlation times of 1.0×10^{-13} s, as this has been determined earlier for similar compounds[27]. For the graphic representation, the plot program SCHAKAL[30] was used. Scatter plots were produced by our own software employing the NCAR graphics library[31].

RESULTS AND DISCUSSION

Synthesis.—Synthesis of the four title compounds employed the known *N*-9-fluorenylmethyl chloroformate (Fmoc) protected benzyl ester derivatives[8] of L-serine

and L-threonine. The monosaccharide derivatives were synthesised via silver trifluoromethanesulfonate (triflate)-mediated coupling[32] of 2,3,4,6-tetra-*O*-acetyl-α-D-mannopyranosyl chloride to protected L-serine and L-threonine derivatives, to give **5** and **6** in 89 and 90% yield, respectively. Deprotection of **5** and **6** in three steps, removal of the Fmoc group with morpholine[11], catalytic hydrogenolysis to remove the benzyl ester, and finally *O*-deacetylation with hydrazine hydrate[33] gave **1** and **2** in 51 and 70% yield, respectively. No racemisation of amino acids was found, according to the ^{1}H- and ^{13}C-NMR spectra, with the conditions described for deprotection. The reason for the discrepancy between the optical rotations for **1** and **2** (measured several times and for different batches) and the literature values[10] is unclear.

The disaccharide ethyl thioglycoside **9** was used as glycosyl donor for the synthesis of the title disaccharide compounds. It was obtained in 80% yield from silver triflate-promoted coupling between ethyl 3,4,6-tri-*O*-benzyl-1-thio-α-D-mannopyranoside (**8**) and 2,3,4,6-tetra-*O*-benzyl-D-mannopyranosyl bromide, the latter prepared via treatment of ethyl 2,3,4,6-tetra-*O*-benzyl-1-thio-α-D-mannopyranoside (**7**) with bromine.

Methyl triflate-assisted coupling[34] between **9** and protected L-serine gave 75% of the α-derivative **10**, together with 14% of the β anomer, whereas coupling between **9** and the secondary hydroxyl group in L-threonine afforded only the α anomer **11** (80% yield). Deprotection of **10** and **11** *via* treatment with morpholine followed by catalytic hydrogenolysis gave the target compounds, **3** and **4**, in 71 and 69% yield, respectively.

Metropolis Monte Carlo (MMC) simulations and calculation of global minima.— Potential energy calculations were performed on compounds **3** and **4**, using a modified version of the GESA program[14,15] also including a MMC simulation routine[20]. MMC simulations lend themselves well to sample the complete conformational space of a saccharide, a difficult task applying a systematic grid search[20]. For the compounds studied, the ϕ and ψ angles at the glycosidic linkages, as well as the ω angles for the hydroxymethyl side-chains, were treated as flexible parameters in the simulations. The χ angles determining the amino acid side-chain conformation of L-serine and L-threonine were kept fixed at 60°, since this orientation can be deduced from the vicinal coupling constants for the coupling between the protons on Cα and Cβ in **3** and **4**. The Pachler-equations[35,36] allow an estimation of the population of *gauche* conformers with χ 60°. From the observed coupling constants, it can be concluded that the amount of *gauche* rotamers with χ 60° is $> 70\%$ for all compounds under investigation. The assumed, preferred orientation of L-serine and L-threonine is also in accordance with recent NMR investigations on related glycopeptides[37] and is supported by the crystal structure of α-D-Man*p*-(1 → O)-L-Thr[25]. Another set of simulations was carried out with χ flexible in order to explore the steric requirement of the amino acid residues and to rule out possible effects of flexibility at the Cα–Cβ bond on the size of $\langle NOE \rangle_{MMC}$ values. It was found that rotation around the Cα–Cβ

bonds does not influence the conformer equlibria at the (1 → 2) and the (1 → O) glycosidic linkages in **3** and **4** to a significant extent. Accordingly, the effect for the NOEs to be discussed below was vanishingly small. For the L-threonine-linked disaccharide **4**, it turned out that the energy barriers at the Cα–Cβ bond were too high to be surmounted with temperature parameters at 300 or 310 K. Only at elevated temperature (900 K) could the complete range of χ values be sampled. This finding suggests more flexibilty for the L-serine-linked disaccharide **3** at this particular bond.

Global minima calculated with GESA were found to have dihedral angles of ϕ_1 −50°, ψ_1 −18°, ϕ_2 −54°, ψ_2 117° for **3**, and ϕ_1 −50°, ψ_1 −20°, ϕ_2 −42°, ψ_2 113° for **4**. Starting with the global minimum conformations, MMC simulations were performed which allowed the calculation of ensemble-average $\langle NOE \rangle_{MMC}$ values (Table I) as well as ensemble-average inter-residue atomic distances (Table II). Analogous data for comparison were derived from the global minimum conformations of **3** and **4** (Tables I and II), enabling an assessment of the relevance of introducing molecular flexibility into the theoretical conformational model. The results of the MMC simulations are best represented by scatter plots (Fig. 1) reflecting the fraction of the total conformational space sampled during the simulation[20]. The scatter plots in Fig. 1(a)–(d) show the sampling of the energy surfaces at the α-(1 → 2) linkages and at the linkages between the mannopyranosyl residues and L-serine and L-threonine in **3** and **4**, respectively. Dots mark the conformational states visited during the simulation and a high dot density (dark shading) therefore indicates regions of low energy. A comparison of the scatter plots for the α-(1 → 2) linkages in **3** and **4** with plots published for the disaccharide α-D-Man*p*-(1 → 2)-α-D-Man*p*-OMe[20] clearly indicates that attachment of the amino acids L-serine or L-threonine to the α-D-mannopyranosyl residue only has a very minor influence on the conformer distribution at the glycosidic linkage between the two α-D-mannopyranosyl residues. This finding is well supported by experimental results (see below). The glycosidic linkages involving the amino acids exhibit scatter plots that indicate more conformational freedom, especially in the ψ-direction, for the linkage to L-serine, in comparison to the linkage to L-threonine. This result is not surprising, since the methyl group in L-threonine retards the rotation at the glycosidic linkage.

NOE experiments.—Irradiation, using NOE difference spectroscopy, at the resonance frequencies of H-1′, H-2′, H-1, and H-2, for both **3** and **4**, resulted in intra- and inter-residue NOEs. Theoretical steady-state $\langle NOE \rangle_{MMC}$ values were calculated on the basis of ensemble-average relaxation matrices, based upon both $\langle r^{-3} \rangle^2$ and $\langle r^{-6} \rangle$ values, derived from the MMC simulations. In addition, the minimum energy conformations of **3** and **4** were used to set up relaxation matrices that yield NOEs corresponding to a single-state conformational model. Both experimental and theoretical derived NOE data are given in Table I.

The dominant inter-glycosidic NOE for both glycopeptides **3** and **4** was that observed for H-2 upon irradiation of H-1′. The intra-glycosidic NOE of H-2′ was

TABLE I

NOEs observed for α-D-mannopyranosyl-(1 → 2)-α-D-mannopyranosyl linked to L-serine (**3**) and L-threonine (**4**), and the corresponding calculated values for the minimum energy conformer, using motional averaging

	Irr. [b]	Obs.	Observed NOE [a]		Calculated NOE					
					Min. NOE		$\langle r^{-6} \rangle$ [c]		$\langle r^{-3} \rangle^2$ [c]	
			Abs.	Rel. [d]	Abs.	Rel.	Abs.	Rel.	Abs.	Rel.
3	H-1 [e]	H-2′	10.2* [f]		9.4*		9.3*		9.3*	
		H-2	8.5	83	7.0	74	9.5	102	9.2	99
	H-2′	H-1′	8.1*		9.3*		7.5*		7.8*	
		H-3′	13.2	163	11.3	122	11.3	151	11.4	146
	H-1	H-2	5.0*		5.8*		5.1*		5.3*	
		Hα	[g]	–	0.0	–	−0.2	–	−0.1	–
		Hβ	3.5	70	4.7	81	4.1	80	4.0	75
		Hβ′	1.0	20	−0.4	−7	0.3	6	0.2	4
		H-5′	5.6	112	9.3	160	8.6	169	8.4	158
	H-2	H-1	5.5*		3.8*		4.2*		4.5*	
		H-1′	16.0	291	11.1	292	13.5	321	13.3	296
		H-3	[h]	–	11.4		11.4		11.4	
	SDEV [i]				1.8	29	1.4	29	1.3	22
4	H-1′	H-2′	10.0*		9.4*		9.3*		9.3*	
		H-2	8.0	80	6.8	72	9.3	100	9.1	98
	H-2′	H-1′	6.0*		9.5*		7.6*		7.9*	
		H-3′	10.3	172	11.4	120	11.3	148	11.4	144
	H-1	H-2	4.6*		5.8*		5.1*		5.4*	
		Hβ′	8.6	187	7.8	134	8.5	167	8.4	155
		Hα	[g]		−0.5	–	−0.6	–	−0.6	–
		H-5′	5.8	126	8.6	148	8.1	159	8.0	148
	H-2	H-1	3.4*		4.4*		4.6*		4.9*	
		H-1′	12.0	355	10.9	248	13.4	291	13.1	267
	SDEV				1.7	58	1.3	36	1.3	45

[a] Average value from two separate experiments; the average error for the observed NOE is within ±10%, and the average error for the relative NOEs is ±14%. [b] Samples were pre-irradiated for 5 s at the frequency of the signals for respective protons. [c] Motional average values derived from $\langle r^{-6} \rangle$ or $\langle r^{-3} \rangle^2$ relaxation matrices. [d] Relative NOE = 100×NOE/NOE*. (reference value). [e] Primed protons belong to the mannopyranosyl group, unprimed to the mannopyranosyl residue, and protons designed as Hα, Hβ, and Hγ to the amino acid residue. [f] The values marked with * are used as NOE reference values for calculation of relative NOE. [g] This signal could not be detected. [h] No quantification could be performed as the observation frequency is too close to the irradiation frequency. [i] The standard deviation was calculated according to $SDEV^2 = 1/N \Sigma(NOE_{obs} - NOE_{calc})^2$.

TABLE II

Short inter-residue atomic distances [a] in compounds **3** and **4**

Atom pair	**3**		**4**	
	$\langle r \rangle$	r	$\langle r \rangle$	r
H-1′–O-3	2.9	2.6	2.9	2.6
H-1′–H-2	2.4	2.5	2.4	2.5
H-5′–H-1	2.4	2.2	2.4	2.2
O-5′–H-1	3.3	3.5	3.3	3.5
O-5′–H-2	2.8	2.6	2.8	2.6
H-1–O(COO)	3.7	2.6	3.0	2.7
H-1–Hβ′	2.4	2.3	2.4	2.4
H-1–Hβ	3.1	3.5		
O-5–Hβ′	3.1	2.6	3.0	2.9
O-5–Hβ	2.9	3.3		

[a] Values $\langle r \rangle$ are derived from MMC simulations, and values r from the global minimum conformations.

larger than the inter-glycosidic NOE of H-2. In former studies of α-D-Man*p*-(1 → 2)-α-D-Man*p*-OMe[24], on larger structures containing this disaccharide element[38,39], and on stereochemically identical disaccharide fragments[21], the analogous NOE experiment gave instead an inter-glycosidic NOE of H-2 that was larger than the simultaneously observed intra-glycosidic NOE of H-2′. In order to examine whether the reverse ordering of these two NOEs originates from interactions of the sugar units with the charged amino or carboxyl groups of L-serine and L-threonine, NOE experiments were performed on compound **4** at a different pD value (pD = 9). The relative sizes of the two NOEs did not change more than ±10% upon variation of pD, thus suggesting that, for the glycopeptides under investigation, charge interactions are not influential on the conformation of the remote α-(1 → 2)-glycosidic linkage. Either anisotropic motion[29] or relaxation pathways for H-2 different from those present in the corresponding disaccharide unit not attached to either L-serine or L-threonine could account for the observed effect.

Irradiation of H-2 in disaccharide **3** resulted in an inter-glycosidic NOE of H-1′ and an intra-glycosidic NOE of H-1 and H-3. However, the NOE observed for H-3 cannot be quantified since the resonance frequencies of H-2 and H-3 are too close. The analogous experiment on the L-threonine-linked disaccharide **4** is not suitable for quantification since the H-2 and H-3 resonances severely overlap and selective irradiation of H-2 was impossible.

Both the dynamic and the static model qualitatively fit the experimental data in terms of absolute and relative NOE values. However, a close inspection of Table I demonstrates that the fit between experimental and theoretical NOE data is improved for both **3** and **4** when utilising $\langle \mathrm{NOE} \rangle_{\mathrm{MMC}}$ values instead of global minimum NOEs. A comparison of ensemble-average $\langle \mathrm{NOE} \rangle_{\mathrm{MMC}}$ values with those derived from the global minimum conformations allowed evaluation of the influence of flexibility around glycosidic linkages on the size of the NOEs and to

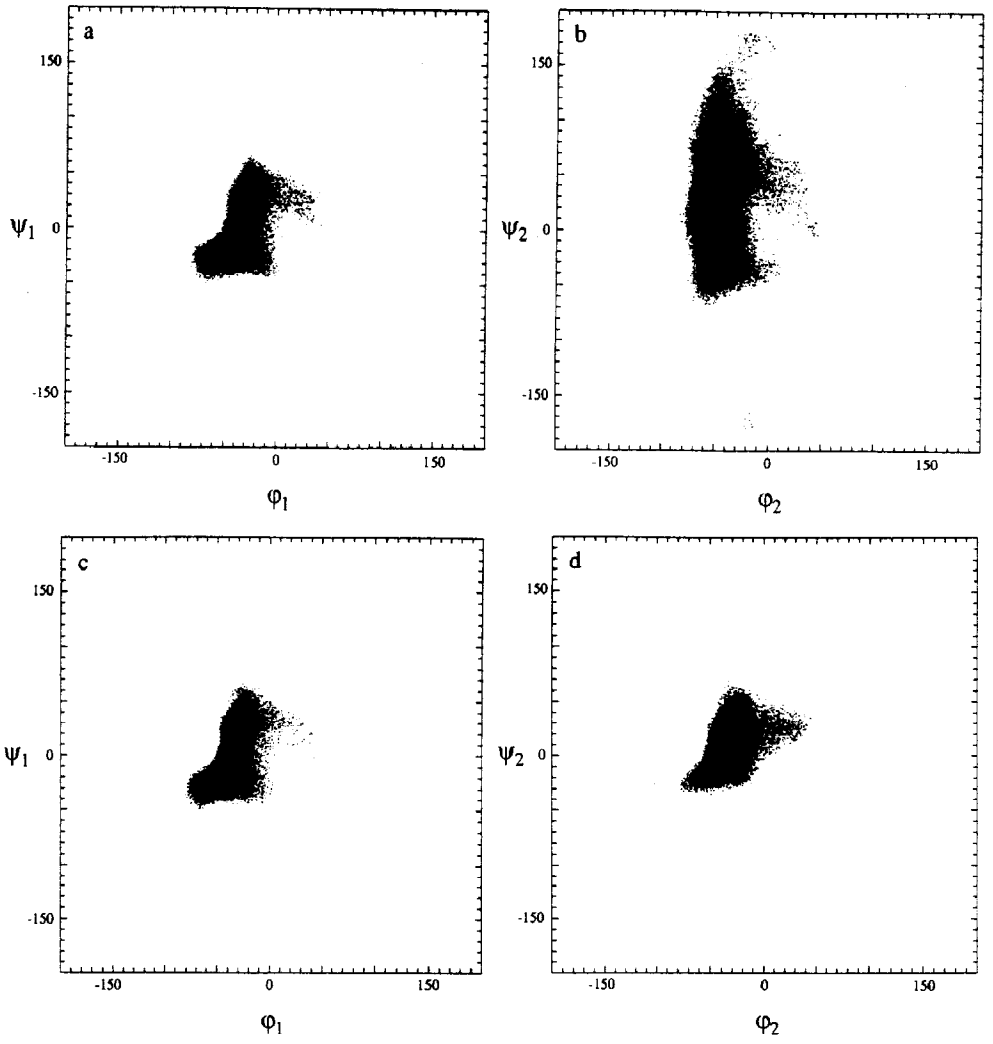

Fig. 1. Scatter plots for the MMC simulations of disaccharides **3** and **4**. Temperature parameters were set at 310 K and 250000 macro moves were performed. All dihedral angles ϕ, ψ, ω, and χ were varied, giving rise to a seven-dimensional conformational hyperspace. The plots represent projections into two-dimensional conformational subspaces. Maximum step lengths were set at 10°, leading to overall acceptance ratios of 0.54 and 0.42 for **3** and **4**, respectively: (a) α-D-Man*p*-(1 → 2)-α-D-Man*p*-(1 → O)-L-Ser, (1 → 2) linkage; (b) α-D-Man*p*-(1 → 2)-α-D-Man*p*-(1 → O)-L-Ser, (1 → O) linkage; (c) α-D-Man*p*-(1 → 2)-α-D-Man*p*-(1 → O)-L-Thr, (1 → 2) linkage; (d) α-D-Man*p*-(1 → 2)-α-D-Man*p*-(1 → O)-L-Thr, (1 → O) linkage.

trace those NOEs that are sensitive towards this flexibility. Inspection of Table I at first sight suggests that theoretical NOEs, with or without taking into account molecular motion around the glycosidic linkage, satisfactorily approach the experimental values. However, analysis of the results in more detail provides evidence that the incorporation of molecular flexibility at the glycosidic bonds into the

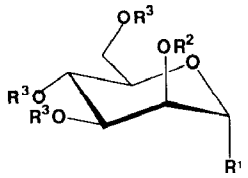

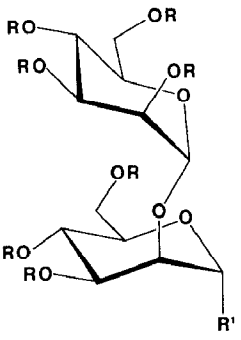

1 R^3=R^2=H, R^1=O-L-serine
2 R^3=R^2=H, R^1=O-L-threonin
5 R^3=R^2=Ac, R^1=O-(*N*-Fmoc-L-serine benzyl ester)
6 R^3=R^2=Ac, R^1=O-(*N*-Fmoc-L-threonine benzyl ester)
7 R^3=R^2=Bn, R^1=SEt
8 R^3=Bn, R^2=H, R^1=SEt

3 R=H, R^1=O-L-serine
4 R=H, R^1=O-L-threonine
9 R=Bn, R^1=O-SEt
10 R=Bn, R^1=O-(*N*-Fmoc-L-serine benzyl ester)
11 R=Bn, R^1=O-(*N*-Fmoc-L-threonine benzyl ester)

theoretical calculations gives a better fit to experimental data. The fit can be quantified by calculating the standard deviations of the theoretically derived NOEs from the corresponding experimental values. The standard deviations, denoted as SDEV, are summarised in Table I. The values support the MMC approach vs. the global minimum model. By comparing global minimum NOEs to $\langle NOE \rangle_{MMC}$ values (Table I), it is also evident that the NOE of H-2 when H-1′ is irradiated is most sensitive towards flexibility around the α-(1 → 2)-glycosidic linkage.

Utilising $\langle NOE \rangle_{MMC}$ values instead of NOEs derived from the global minimum, a better agreement between theoretical and experimental data was also accomplished when H-2′ was irradiated for both glycopeptides **3** and **4**. Although there are no inter-glycosidic NOEs, the two enhancements of H-1′ and H-3′ are clearly influenced by relaxation pathways to remote protons across the glycosidic linkage. Especially, the size of the NOE of H-1′ is influenced by inter-glycosidic dipolar interactions, mainly to H-2. Therefore, the experiment also supports the assumption that flexibility around glycosidic linkages cannot be neglected.

Irradiation of H-1 (Figs. 2b and 3b) leads to inter-glycosidic NOEs of H-5′, Hβ, and Hβ′ in **3** and H-5′ and Hβ in **4**, in qualitative agreement with NOEs predicted from the MMC simulation as well as from the global minimum conformations, but a quantitative comparison reveals that the MMC-derived $\langle NOE \rangle_{MMC}$ values again give a closer fit to the experimental data. Special care has to be taken when discussing the NOE observed for H-5′. This NOE is calculated to be too large in both **3** and **4**, compared to the experimentally observed value, which could

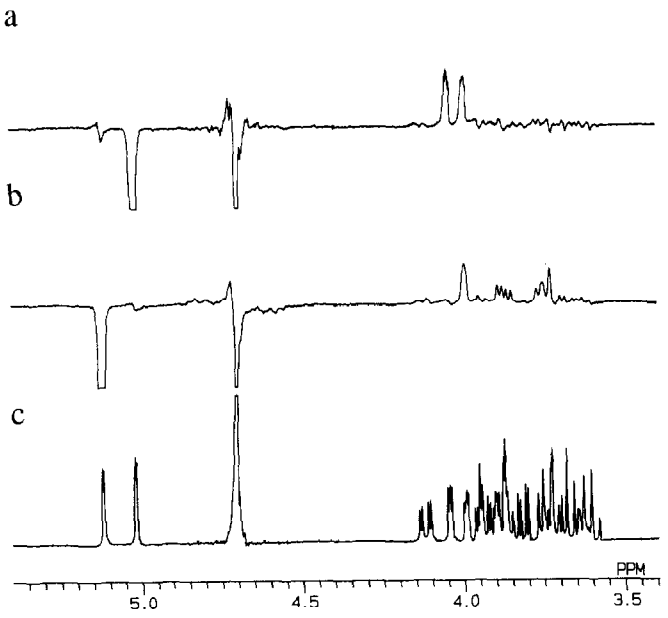

Fig. 2. NOE difference spectra obtained with irradiation at the resonance frequencies of H-1′ (a) and H-1 (b), and the ^{1}H-NMR spectrum (c) of **3**.

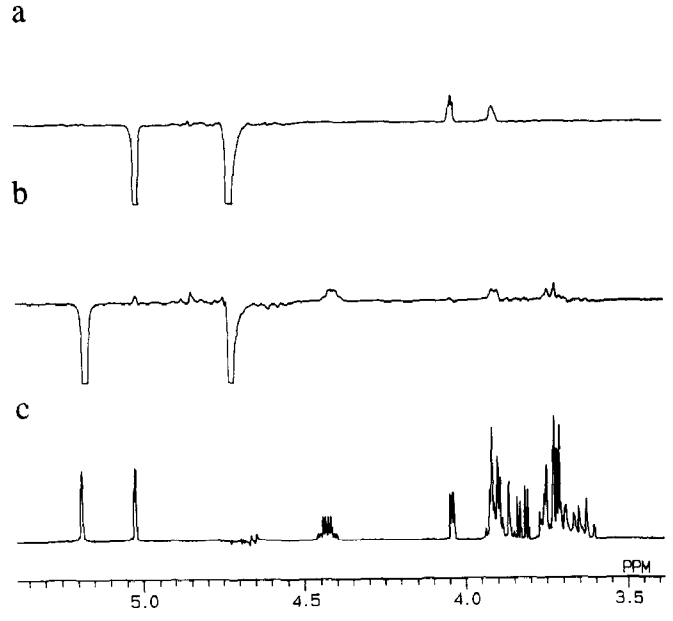

Fig. 3. NOE difference spectra obtained with irradiation at the resonance frequencies of H-1′ (a) and H-1 (b), and the ^{1}H-NMR spectrum (c) of **4**.

be due to the fact that no extra torsional potential function was used for the rotation around the C-5–C-6 bonds.

^{1}H-NMR chemical shift data.—The ^{1}H-NMR chemical shifts of signals for compounds **1–4** and corresponding data for the constituent monomers are given in Table III. Chemical shift differences were calculated for all compounds relative to the monomers α-D-mannopyranose, L-serine, and L-threonine. For **3** and **4**, chemical shift differences were also calculated relative to the disaccharide α-D-Man*p*-(1 → 2)-α-D-Man*p*-OMe in order to separate effects due to amino acid attachment from those caused by linking a second α-D-mannopyranosyl group to O-2 of the α-D-mannopyranosyl residue linked to the amino acids. Likewise, chemical shift differences were calculated for the signals from the latter α-D-mannopyranosyl residues and the attached L-serine and L-threonine in **3** and **4** relative to those from the corresponding compounds **1** and **2**, in order to unravel effects of the terminal α-D-mannopyranosyl group.

Distances (Table II) found for the global minimum conformations of **3** and **4**, and corresponding short ensemble-average distances taken from the MMC simulations were used to explain the chemical shift differences. Comparison of the chemical shifts for signals from **1** and **2** with those from their monomeric building units (Table III, values in parentheses) reveals effects due to the glycosylation of the amino acid residues. Significant upfield shifts were observed for the signals from H-1 and H-5, and downfield shifts for the signals from Hα and Hβ. The upfield shift of the signal from H-1 in **1** and **2** corresponds to a proximity between H-1 and Hβ in the attached amino acid (Table II). The average orientation of the oxygen atom involved in the glycosidic linkage must be altered compared to its orientation in α-D-mannopyranose and this should influence the chemical shift for protons close to this oxygen. Accordingly, an upfield shift is observed for H-5, which is in a 1,3-diaxial relation to the glycosidic oxygen O-1 in both glycopeptides **1** and **2**. This shift is more pronounced in **1** than in **2**, which could indicate different conformer distributions at the glycosidic linkage to L-serine compared to that to L-threonine. A comparison with the scatter plots for these linkages (Fig. 1b and 1d) shows that this finding is in accordance with the results of the MMC simulations, indicating more flexibility for the linkage to L-serine. Almost the same effects can be observed when comparing chemical shift values of the 2-*O*-substituted α-D-mannopyranosyl residue of α-D-Man*p*-(1 → 2)-α-D-Man*p*-OMe with the corresponding values for **3** and **4** (see Table III, values in {brackets}).

The overall conclusion to be drawn is that the attachment of the second α-D-mannopyranosyl group does not influence the conformational equilibrium at the glycosidic linkage to the amino acid to a significant extent. This deduction is substantiated by the observation that the chemical shift values found for the terminal α-D-mannopyranosyl group in α-D-Man*p*-(1 → 2)-α-D-Man*p*-OMe are almost identical with those for **3** and **4**. Summarising these experimental observations, it can be inferred that the two glycosidic linkages do not mutually alter the conformational equilibria at either linkage. Comparing the scatter plots (Fig. 1a

^{1}H-NMR chemical shifts for signals from compounds **1–4** and appropriate monomers obtained at 30° and pD ~ 5 [a]

Compound	H-1	H-2	H-3	H-4	H-5	H-6a	H-6b	Hα	Hβ	Hβ′	Hγ
α-D-Man*p*-(1 →	4.87	3.98	3.84	3.65	3.65	3.91	3.76				
	(−0.30)	(0.06)	(0.00)	(0.00)	(−0.16)	(0.04)	(0.01)				
→ O)-L-Ser (**1**)								3.97	4.12	3.90	
								(0.13)	(0.14)	(−0.04)	
α-D-Man*p*-(1 →	4.91	3.88	3.80	3.63	3.73	3.87	3.74				
	(−0.26)	(−0.04)	(−0.04)	(−0.02)	(−0.08)	(0.00)	(−0.01)				
→ O)-L-Thr (**2**)								3.72	4.45		1.41
								(0.14)	(0.20)		(0.09)
α-D-Man*p*-(1 →	5.02	4.06	3.83	3.62	3.76	3.90	3.72				
	(−0.15)	(0.14)	(−0.01)	(−0.03)	(−0.05)	(0.03)	(−0.03)				
	{0.00}	{0.00}	{−0.01}	{0.00}	{0.00}	{0.01}	{0.00}				
→ 2)-α-D-Man*p*-(1 →	5.12	4.00	3.95	3.69	3.64	3.91	3.77				
	(−0.05)	(0.08)	(0.11)	(0.04)	(−0.17)	(0.04)	(0.02)				
	[0.25]	[0.02]	[0.11]	[0.04]	[−0.01]	[0.00]	[0.01]				
	{0.13}	{0.05}	{0.09}	{0.01}	{0.04}	{0.01}	{0.01}				
→ O)-L-Ser (**3**)								3.97	4.12	3.88	
								(0.13)	(0.14)	(−0.06)	
								[0.00]	[0.00]	[−0.02]	
α-D-Man*p*-(1 →	5.02	4.04	3.83	3.63	3.74	3.91	3.73				
	(−0.15)	(0.12)	(−0.01)	(−0.02)	(−0.07)	(0.04)	(−0.02)				
	{0.00}	{0.02}	{−0.01}	{−0.01}	{−0.02}	{0.02}	{0.01}				
→ 2)-α-D-Man*p*-(1 →	5.19	3.92	3.91	3.66	3.71	3.88	3.74				
	(0.02)	(0.00)	(0.07)	(0.01)	(−0.10)	(0.01)	(−0.01)				
	[0.28]	[0.04]	[0.11]	[0.03]	[−0.02]	[0.01]	[0.00]				
	{0.20}	{−0.02}	{0.05}	{−0.02}	{0.11}	{−0.02}	{−0.02}				
→ O)-L-Thr (**4**)								3.73	4.43		1.40
								(0.15)	(0.18)		(0.08)
								[0.01]	[−0.02]		[−0.01]
α-D-Man*p*-(1 →	5.02	4.06	3.84	3.62	3.76	3.89	3.72				
→ 2)-α-D-Man*p*-OMe	4.99	3.95	3.86	3.68	3.60	3.90	3.76				
α-D-Man*p*	5.17	3.92	3.84	3.65	3.81	3.87	3.75				
L-Ser								3.84	3.98	3.94	
L-Thr								3.58	4.25		1.32

[a] Chemical shift differences are calculated by subtraction of chemical shifts for signals of α-D-mannose and L-serine or L-threonine (parentheses) from those of the corresponding residues in compounds **1–4**. Values in [brackets] represent chemical shift differences for signals of **3** and **4** relative to those of the corresponding residues in compounds **1** and **2**. For the disaccharide peptides, chemical shift differences of the mannopyranosyl residues are also given relative to the chemical shifts of α-D-Man*p*(1 → 2)-α-D-Man*p*-OMe {brackets}. A positive difference indicates a downfield shift.

and 1c) for the α-(1 → 2)-glycosidic linkages in **3** and **4** to each other and to that for α-D-Man*p*-(1 → 2)-α-D-Man*p*-OMe[20] shows that there are almost no alterations in shape, which is in excellent agreement with these experimental results.

A comparison of the chemical shift values of the 2-*O*-substituted mannopyranosyl residues in **3** and **4** with those of α-D-mannopyranose (Table III, values in parentheses) and with those found for the α-D-mannopyranosyl group of monosaccharide derivatives **1** and **2** (Table III, values in [brackets]) uncovers the effects of the formation of the α-(1 → 2)-glycosidic linkage. Significant downfield shifts (> 0.05 ppm) are observed for signals from H-1′, H-2′, H-5′, H-1, and H-3. These effects are identical to those described for α-D-Man*p*-(1 → 2)-α-D-Man*p*-OMe in a recent study[24] and will not be discussed any further at this point. It should be emphasised, though, that the large downfield shift of the H-1 resonance does not correspond to a close contact between H-1 and O-5′, as suggested earlier[40]. Neither the global minimum conformations nor the MMC simulation can support this suggestion, since this distance is found to be 3.5 Å for the global minimum conformations of **3** and **4**, and a value of 3.3 Å is found when averaging the distances from the MMC simulation of **3** and **4**.

The differences in chemical shifts found for signals from the amino acid residues in comparison to those from the free amino acids show large downfield shifts for the signals from all protons but Hβ′. When comparing the chemical shifts of the L-serine and L-threonine proton signals for **1** and **2** to the corresponding values for the disaccharide derivatives **3** and **4** (Table III, values in {brackets}), it is clear that the attachment of a second α-D-mannopyranosyl residue leaves the chemical shift values of the amino acids unchanged, which is in accordance with the discussion above.

^{13}C-NMR chemical shift data.—^{13}C-NMR chemical shifts for **1**–**4**, as well as for relevant monomers, together with chemical shift differences obtained relative to the respective monomers and **1** and **2**, are given in Table IV. A common pattern, with significant chemical shift differences (> 0.5 ppm) for signals from the linkage carbons, the carbons next to these, and C-5 of all α-D-mannopyranosyl residues, is observed. Shift differences observed for **3** and **4** were similar to those found for other (1 → 2)-linked disaccharide methyl glycosides with the *manno* configuration[41]. The chemical shift differences found for the anomeric carbon signals for **1** and **2** reflect the influence of the different amino acids, L-serine and L-threonine. Upon glycosylation with the primary alcohol L-serine, a downfield shift of the C-1 signal of 6.5 ppm is observed (Table IV) for **1** compared to a value of 7.5 ppm for **2** when the secondary alcohol L-threonine is involved. Downfield shifts are observed for the signals from Cβ in **1** and **2**, and the difference between these (2.5 ppm) is larger than that (1.0 ppm) for the signals from the anomeric carbons. It is known that such differences in glycosylation shifts of anomeric carbon signals and the corresponding aglyconic carbon signals reflect differences in the preferred conformations around the glycosidic linkages in question[42]. This observation again supports the results of the MMC simulations, which suggested differences in

TABLE IV

^{13}C-NMR chemical shifts for signals from compounds **1–4** and appropriate monomers obtained at 30° and pD ~ 5 [a]

Compound	C-1	C-2	C-3	C-4	C-5	C-6	COO	Cα	Cβ	Cγ
α-D-Man*p*-(1 →	101.30	70.56	71.15	67.51	73.92	61.80				
	(6.46)	(−0.97)	(0.07)	(−0.19)	(0.69)	(−0.01)				
→ O)-L-Ser (**1**)							172.85	55.46	67.12	
							(−0.23)	(−1.76)	(6.12)	
α-D-Man*p*-(1 →	102.32	70.82	71.07	67.59	74.10	61.86				
	(7.48)	(−0.71)	(−0.01)	(−0.11)	(0.87)	(0.05)				
→ O)-L-Thr (**2**)							172.99	60.01	75.35	19.14
							(−0.53)	(−1.25)	(8.65)	(−1.13)
α-D-Man*p*-(1 →	102.96	70.80	71.17	67.72	74.10	61.97				
	(8.12)	(−0.73)	(0.09)	(0.02)	(0.87)	(0.16)				
→ 2)-α-D-Man*p*-(1 →	99.73	79.07	70.80	67.72	73.98	61.81				
	(4.89)	(7.54)	(−0.28)	(0.02)	(0.75)	(0.00)				
	[−1.57]	[8.51]	[−0.35]	[0.21]	[0.06]	[0.01]				
→ O)-L-Ser (**3**)							172.69	55.43	67.40	
							(−0.39)	(−1.79)	(6.40)	
							[−0.16]	[−0.03]	[0.28]	
α-D-Man*p*-(1 →	102.86	70.82	71.19	67.77	74.06	61.94 [b]				
	(8.02)	(−0.71)	(0.11)	(0.07)	(0.83)	(0.13)				
→ 2)-α-D-Man*p*-(1 →	100.61	79.23	70.77	67.79	74.14	61.90 [b]				
	(5.77)	(7.70)	(−0.31)	(0.09)	(0.91)	(0.09)				
	[−1.74]	[8.41]	[−0.30]	[0.20]	[0.04]	[0.04]				
→ O)-L-Thr (**4**)							172.71	60.01	75.45	19.06
							(−0.81)	(−1.25)	(8.75)	(−1.21)
							[−0.18]	[0.00]	[0.10]	[−0.08]
α-D-Man*p*-(1 →	102.88	70.95	71.50	68.00	74.16	62.19 [b]				
→ 2)-α-D-Man*p*-OMe	100.50	78.88	71.35	68.22	73.64	62.01 [b]				
α-D-Man*p*	94.84	71.53	71.08	67.70	73.23	61.81				
L-Ser							173.08	57.22	61.00	
L-Thr							173.52	61.26	66.70	20.27

[a] Chemical shift differences are calculated by subtraction of chemical shifts for signals of the corresponding α-D-mannose and free amino acid (parentheses) or corresponding residue in compounds **1** and **2** [brackets] from those of the mannopyranosyl and substitued amino acid residues, respectively. A positive difference indicates a downfield shift. [b] The assignments can be interchanged.

flexibility and thus conformer distribution at the glycosidic linkage between the α-D-mannopyranosyl residue and L-serine and L-threonine (Fig. 1b and 1d).

When compounds **1** and **2** are substituted with an additional α-D-mannopyranosyl group to give **3** and **4**, the C-1, C-2, and C-3 signals of the 2-*O*-substituted residue are shifted ~ −1.6, ~ 8.5, and ~ −0.3 ppm, respectively, with only minor differences between **3** and **4**. The signals from the amino acid residues are shifted to an insignificant extent. This finding indicates that no major conformational changes at the glycosidic linkages to the amino acid residues are brought about by adding a second α-D-mannopyranosyl group. The chemical shifts of the signals from **1** and **2** for solutions in H_2O have been reported earlier[43], and only a shift for the signals due to the different solvent and reference value is obtained.

CONCLUSIONS

The conformational analysis performed for the synthetic model compounds **1–4** allows the conclusion that the two glycosidic linkages do not mutually influence the distribution of conformers at either linkage to an extent that could be verified experimentally. Interactions of the carbohydrate part and the attached amino acids were detected only for the α-D-mannopyranosyl residue directly linked to the amino acid. The use of MMC simulations instead of simple global minimum models to yield ensemble-average NMR parameters, such as NOEs, was beneficial for the interpretation of experimental NMR data by allowing the restricted conformation space spanned by the exocyclic dihedral angles in disaccharides **3** and **4** to be sampled conveniently. From the experiments and the calculations, it can be concluded that the linkage between D-mannose and L-serine is more flexible than the linkage between D-mannose and L-threonine. To illustrate those results, the global minimum conformations for the glycopeptides **3** and **4** are shown

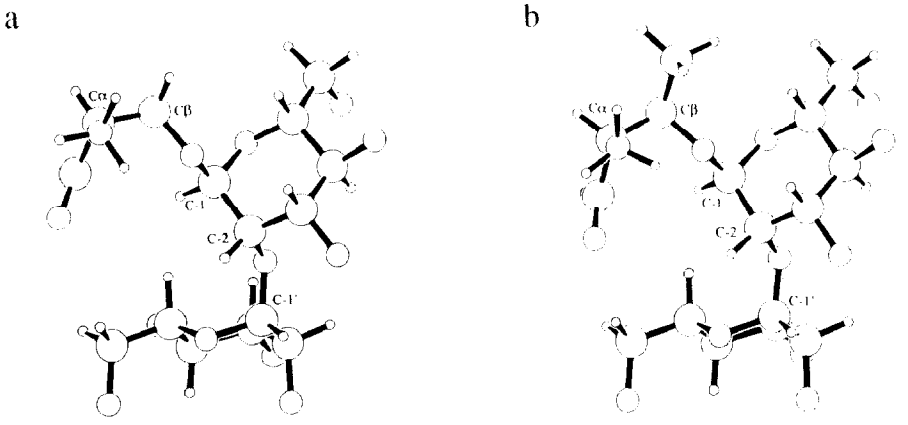

Fig. 4. Representations of the global minimum conformers of disaccharides **3** and **4**. The dihedral angles are as given in the text.

in Fig. 4. They represent a family of similar low-energy conformations. The amount of flexibility at the glycosidic linkages can be deduced from the scatter plots in Fig. 1. The conformational studies performed clearly support a line of evidence showing that Metropolis Monte Carlo simulation techniques provide a well suited method for the interpretation of experimental NMR results for saccharides and glycopeptides in aqueous solution and that incorporation of molecular flexibility at the glycosidic bonds into the theoretical calculations is warranted.

ACKNOWLEDGMENTS

This work was supported by grants from the Swedish Natural Science Research Council and The Swedish National Board for Technical Development. T.P. and J.R.B. thank the NATO for a research grant CRG.890356.

REFERENCES

1 J. Montreuil, *Adv. Carbohydr. Chem. Biochem.*, 37 (1980) 157–223.
2 A. Gunnarsson, B. Svensson, B. Nilsson, and S. Svensson, *Eur. J. Biochem.*, 145 (1984) 463–467.
3 P. Gellerfors, K. Axelsson, A. Helander, S. Johansson, L. Kenne, S. Lindqvist, B. Pavlu, A. Skottner, and L. Fryklund, *J. Biol. Chem.*, 264 (1989) 11444–11449.
4 J.F.G. Vliegenthart, L. Dorland, and H. van Halbeek, *Adv. Carbohydr. Chem. Biochem.*, 41 (1983) 209–374.
5 B. Meyer, *Top. Curr. Chem.*, 154 (1990) 141–208.
6 A.M. Jansson, M. Meldal, and K. Bock, *Tetrahedron Lett.*, 31 (1990) 6991–6994.
7 P.J. Garegg, S. Oscarson, and M. Szönyi, *Carbohydr. Res.*, 205 (1990) 125–132.
8 C.D. Chang, M. Waki, M. Ahmad, J. Meienhofer, E.O. Lundell, and J.D. Haug, *Int. J. Peptide Protein Res.*, 15 (1980) 59–66.
9 E. Pacsu, *Ber.*, 61 (1928) 1508–1511.
10 A.A. Pavia, S.N. Ung-Chhun, and J.-M. Lacombe, *Nouv. J. Chim.*, 5 (1981) 101–108.
11 P. Schultheiss-Reimann and H. Kunz, *Angew. Chem. Suppl.*, (1982) 39–46.
12 J. Fried and D.E. Walz, *J. Am. Chem. Soc.*, 71 (1949) 140–143.
13 E.S. Rachaman, R. Eby, and C. Schuerch, *Carbohydr. Res.*, 67 (1978) 147–161.
14 B. Meyer, *Int. Carbohydr. Symp., XIth, Vancouver, 1982*, Abstr. II/25.
15 H. Paulsen, T. Peters, V. Sinnwell, R. Lebuhn, and B. Meyer, *Liebigs Ann. Chem.*, (1984) 951–976.
16 R.U. Lemieux, K. Bock, L.T.J. Delbaere, S. Koto, and V.S. Rao, *Can. J. Chem.*, 58 (1980) 631–653.
17 H. Thøgersen, R.U. Lemieux, K. Bock, and B. Meyer, *Can. J. Chem.*, 60 (1981) 44–57.
18 R.U. Lemieux, A.A. Pavia, J.C. Martin, and K.A. Watanabe, *Can. J. Chem.*, 47 (1969) 4427–4439.
19 J.-P. Praly and R.U. Lemieux, *Can. J. Chem.*, 65 (1987) 213–223.
20 T. Peters, B. Meyer, R. Stuike-Prill, R. Somorjai, and J.-R. Brisson, *Carbohydr. Res.*, submitted.
21 T. Peters J.-R. Brisson, and D.R. Bundle, *Can. J. Chem.*, 68 (1990) 979–988.
22 D.A. Cumming and J.P. Carver, *Biochemistry*, 26 (1987) 6664–6676.
23 A. Imberty, V. Tran, and S. Pérez, *J. Comput. Chem.*, 11 (1989) 205–216.
24 T. Peters, *Liebigs Ann. Chem.*, (1991) 135–144.
25 N. Darbon, Y. Oddon, J.-M. Lacombe, and A.A. Pavia, *Carbohydr. Res.*, 130 (1984) 55–64.
26 G.A. Jeffrey, R.K. McMullan, and S. Takagi, *Acta Crystallogr., Sect. B*, 33 (1977) 728–733.
27 J.-R. Brisson and J.P. Carver, *Biochemistry*, 22 (1983) 1362–1368.
28 F. Heatley, L. Akhter, and R.T. Brown, *J. Chem. Soc., Perkin Trans. 2*, (1980) 919–924.
29 K. Bock, H. Lönn, and T. Peters, *Carbohydr. Res.*, 198 (1990) 375–380.
30 E. Keller, SCHAKAL-88B, Plot Program, University of Freiburg, 1988.
31 NCAR–Graphics, Version 3.0, December 1989, Scientific Computing Division, National Center for Atmospheric Research, Boulder, Colorado.

32 S. Hanessian and J. Banoub, *Carbohydr. Res.*, 53 (1977) C13–C16.
33 H. Kunz and H. Waldmann, *Helv. Chim. Acta*, 68 (1985) 618–622.
34 H. Lönn, *Carbohydr. Res.*, 139 (1985) 115–121.
35 K.G.R. Pachler, *Spectrochim. Acta*, 20 (1964) 581–587.
36 A. DeMareo, M. Llinás, and K. Wüthrich, *Biopolymers*, 17 (1978) 617–636.
37 H. Paulsen, A. Pollex-Krüger, and V. Sinnwell, *Carbohydr. Res.*, 214 (1991) 199–226.
38 S.W. Homans, A. Pastore, R.A. Dwek, and T.W. Rademacher, *Biochemistry*, 26 (1987) 6649–6655.
39 C.J. Edge, U.C. Singh, R. Bazzo, G.L. Taylor, R.A. Dwek, and T.W. Rademacher, *Biochemistry*, 29 (1990) 1971–1974.
40 T. Ogawa and K. Sasajima, *Carbohydr. Res.*, 97 (1981) 205–227.
41 P.-E. Jansson, L. Kenne, and H. Ottosson, *J. Chem. Soc., Perkin Trans. 1*, (1990) 2011–2018.
42 K. Bock, A. Brignole, and B.W. Sigurskjold, *J. Chem. Soc., Perkin Trans. 2*, (1986) 1711–1713.
43 A. Allerhand, K. Dill, E. Berman, J.M. Lacombe, and A.A. Pavia, *Carbohydr. Res.*, 97 (1981) 331–336.